Spatial, seasonal trends and transboundary transport of PM2.5 inorganic ions in the Veneto region (Northeastern Italy)

Mauro Masiol[a*], Francesca Benetello[b]
Roy M. Harrison[a†], Gianni Formenton[c]
Francesco De Gaspari[c], Bruno Pavoni[b]

Published in
Atmospheric Environment 117 (2015) 19-31

http://dx.doi.org/10.1016/j.atmosenv.2015.06.044

https://www.sciencedirect.com/science/article/abs/pii/S1352231015301862?via%3Dihub

[*] To whom correspondence should be addressed. Email: m.masiol@bham.ac.uk

[†] Also at: Department of Environmental Sciences / Center of Excellence in Environmental Studies, King Abdulaziz University, PO Box 80203, Jeddah, 21589, Saudi Arabia

SPATIAL, SEASONAL TRENDS AND TRANSBOUNDARY TRANSPORT OF $PM_{2.5}$ INORGANIC IONS IN THE VENETO REGION (NORTHEASTERN ITALY)

Mauro Masiol[a*], Francesca Benetello[b]
Roy M. Harrison[a†], Gianni Formenton[c]
Francesco De Gaspari[c], Bruno Pavoni[b]

[a]Division of Environmental Health and Risk Management
School of Geography, Earth and Environmental Sciences
University of Birmingham
Edgbaston, Birmingham B15 2TT
United Kingdom

[b]Dipartimento di Scienze Ambientali
Informatica e Statistica, Università Ca' Foscari Venezia
Dorsoduro 2137, 30123 Venezia, Italy

[c]Dipartimento Provinciale di Padova
Agenzia Regionale per la Prevenzione e Protezione Ambientale del Veneto (ARPAV), Via Ospedale 22, 35121 Padova, Italy

[*] To whom correspondence should be addressed. Email: m.masiol@bham.ac.uk

[†] Also at: Department of Environmental Sciences / Center of Excellence in Environmental Studies, King Abdulaziz University, PO Box 80203, Jeddah, 21589, Saudi Arabia

ABSTRACT

The Veneto Region lies in the eastern part of the Po Valley (Italy). This is one of the hotspots in Europe for air quality, where efforts to meet the European standard for $PM_{2.5}$ according to current and future legislation have been generally unsuccessful. Recent data indicating that ammonium, nitrate and sulphate account for about one third of total $PM_{2.5}$ mass show that secondary inorganic aerosol (SIA) plays a key role in the exceedence of the standards. A sampling campaign for $PM_{2.5}$ was carried out simultaneously in six major cities (2012-2013). The water soluble inorganic ions were quantified and data processed to: (1) investigate the seasonal trends and the spatial variations of the ionic component of aerosol; (2) identify chemical characteristics at the regional-scale and (3) assess the potential effects of long-range transport using back-trajectory cluster analysis and concentration-weighted trajectory (CWT) models. Results indicated that $PM_{2.5}$ and SIA ions have an increasing gradient in concentrations from North (mountain) to South (lowland) and from East (coastal) to West (more continental), whereas K^+ and Ca^{2+} levels are quite uniformly distributed. Similar seasonal trends in $PM_{2.5}$ and ions are seen across the region. Simultaneous daily changes were observed and interpreted as a consequence of similar emission sources, secondary pollutant generation and accumulation/removal processes. Sulphate and nitrate were not directly related to the concentrations of their precursor gases and were generally largely, but not completely, neutralised by ammonium. The clustering of back-trajectories and CWT demonstrate that the long-range movement of the air masses has a major impact upon $PM_{2.5}$ and ion concentrations: an area spreading from Eastern to Central Europe was identified as a main potential source for most ions. The valley sites are also heavily influenced by local emissions in slow moving northerly air masses. Finally, two episodes of high nitrate levels were investigated to explain why some sites are experiencing much higher concentrations than others. This study identifies some key features in the generation of SIA in the Po Valley,

demonstrating that SIA generation is a regional pollution phenomenon and mitigation policies are required at regional, national and even European scales.

Keywords: $PM_{2.5}$, Ionic composition, Secondary inorganic aerosol, Long-range transport, Po Valley

1. INTRODUCTION

Although most elements of the periodic table and many thousands of different organic compounds are found in airborne particulate matter (PM), a few major components usually make up a large percentage of the total mass. Ammonium (NH_4^+), nitrate (NO_3^-) and sulphate (SO_4^{2-}) are among the major components of aerosol in the lower troposphere and their average mass percentages in fine PM (aerodynamic diameter less than 2.5 μm, $PM_{2.5}$) account for ~7%, ~9% and ~15%, respectively in southern Europe (Putaud et al., 2010). These ions can be directly emitted from various sources, including sea salt, mineral dust, traffic, biomass combustion, industries and other anthropogenic processes. However, the dominant mechanisms for their presence in the particulate-phase are the oxidation of precursor gases, i.e. nitrogen oxides ($NO+NO_2=NO_x$) and sulfur dioxide (SO_2), to nitric (HNO_3) and sulfuric (H_2SO_4) acids, respectively. The subsequent neutralisation with ammonia (NH_3) forms salts such as ammonium nitrate (NH_4NO_3), ammonium sulphate ($(NH_4)_2SO_4$) and ammonium bisulphate ($(NH_4)HSO_4$) (Seinfeld and Pandis, 2006; Holmes, 2007; Benson et al., 2011). These salts are commonly referred to as secondary inorganic aerosol (SIA).

$PM_{2.5}$ has clearly demonstrated adverse effects upon human health (WHO, 2006), and reducing human exposure to PM is, therefore, of primary importance. In particular, it is a key objective in the few hot-spots left in Europe, such as the Po Valley, where the current standards for PM are not met. Several large cities (e.g., Milan, Turin, Bologna, Verona and Venice-Mestre) and a myriad of minor urban agglomerations, industrial areas, agricultural and rural environments are spread over a ~$48 \cdot 10^3$ km^2-wide alluvial lowland. A total of ~16 million inhabitants and the related road traffic and energy production cause heavy anthropogenic emissions across the entire valley. In addition, enclosure by the Alps and

Apennine mountains surrounding the valley from the North, West and South (only the eastern side is opened to the Adriatic Sea) forms a barrier for the dispersion of pollutants and has a negative impact on air quality, with a buildup of PM and nitrogen oxides mainly during the cold season. Sampling at a rural site in the south-eastern Po Valley (San Pietro Capofiume), Decesari et al. (2014) found that sulphate and nitrate contributed appreciably to particulate matter mass. Their analysis of the association of particulate matter concentrations with meteorological factors revealed a complex interplay of local and long-range transport influences.

The European Directive 2008/50/EC imposed a $PM_{2.5}$ annual average concentration of 25 μg m^{-3} as a *target* value to be achieved by 2010. As the *target* value will become the European *limit* value to be met by 2015, this standard has to be achieved with the current and future legislation. However this concentration is not met in many locations of Veneto Region, Eastern Po Valley (EEA, 2013): in 2012, eight of the 14 sites included in the main monitoring plan for $PM_{2.5}$ of the local environmental protection agency (ARPAV) breached the target value (ARPAV, 2013). These sites are located in a number of major cities of the region and generally the $PM_{2.5}$ concentrations were 3−7 μg m^{-3} above the target value. In addition, $PM_{2.5}$ levels exceeding the target value were also recorded in rural environments demonstrating that even the background pollution is high.

Almost all the literature available for the SIA pollution in the Veneto is based on studies carried out in the Municipality of Venice (Squizzato et al., 2012;2013; Masiol et al., 2014a). Results have shown that about 25−35% of the total $PM_{2.5}$ mass in Venice-Mestre is made up of SIA, which is therefore a key component when the target values in the eastern Po Valley are exceeded. Consequently, successful policies should include not only the reduction of

direct (primary) sources, but also the reduction of precursor gases to prevent the formation of secondary particles (de Leeuw, 2002; Andreani-Aksoyoglu et al., 2004; Wu et al., 2008).

However, data collected in a single coastal city, Venice, are not sufficient to depict the key characteristics of SIA pollution across the Veneto, the territory of which extends from Alpine environments to foothills to flat plain areas in the North-South axis and extends from continental to coastal environments in the West-East axis.

In view of this, the present study investigates the levels, spatial distribution and sources of SIA in six major cities of Veneto, which have been carefully selected to be representative of different environments of the region. The investigated territory extends to ~125 km on the North-South axis and ~60 km from West to Est. The inorganic ionic composition of $PM_{2.5}$ was quantified at six sites located in major cities for one year (2012−2013). The seasonal and spatial variations were examined using a series of statistical tests and chemometric approaches. Starting from the experimental data, the SIA formation at a regional-scale in Veneto is described and the potential local and external sources are investigated. This study has identified some key features that can improve the understanding of the generation of secondary inorganic particles in the entire Po Valley.

2. MATERIALS AND METHODS

2.1 Site Selection

A multiple-site $PM_{2.5}$ sampling campaign was carried out according to the EN 14907:2005 standard from April 2012 to March 2013 in 6 major cities: Belluno (BL), Conegliano (TV), Vicenza (VI), Venice-Mestre (VE), Padua (PD) and Rovigo (RO) (Figure 1a). Stations managed by ARPAV, were placed in high density residential areas and can be considered as

representative of city-wide background levels. In Table 1 some site characteristics are summarised. Since the Veneto region includes a northern Alpine zone (29% of the territory), an intermediate hilly one (15%), a wide southern flat lowland (56%) and an eastern coastline (95 km long), the cities were also selected to represent most of the differing environments and features of the territory. BL (36,600 inhabitants) is located in an Alpine valley surrounded by mountains, with no large industries or heavy traffic, but biomass burning emissions are intense in winter, as wood is largely used for domestic heating. TV (35,700 inhabitants) is in a foothill region and is therefore representative of the transition between the mountain and lowland; many factories process stainless steel, produce appliances and electrical equipment, but a large part of the land is used for agriculture, especially for vineyards. VI (115,900 inhabitants) is an important city with intense traffic and small to medium-sized mechanical, textile, tanning and jewelry manufactures. VE (271,000 inhabitants) is a conurbation extending from the coastal lagoon of Venice to the mainland with a complex emission scenario. This includes heavy road, maritime and airport traffic, an industrial zone hosting chemical and steel plants, an oil-refinery, incineration facilities, thermoelectric power plants and others. PD (214,200 inhabitants) is the most densely populated municipality of the region, with many medium-sized factories mainly in the engineering, technological and building sectors, but it also suffers from intense traffic due to the presence of a large intermodal and logistics hub. RO (52,800 inhabitants) is located in a flat lowland midway between the Alps and the Apennines and is the biggest processing center of Veneto for agricultural products. Demographic data refer to 2011 and to the whole municipalities.

2.2 Experimental

PM was collected on quartz fiber filters (Whatman QMA), starting at midnight for 24 h continuously using low-volume samplers installed in air conditioned cabins (temperature <20°C). $PM_{2.5}$ masses were gravimetrically determined (sensitivity 0.1 µg) after preconditioning at constant temperature (20±1 °C) and relative humidity (50±5%). Sampled filters were stored in clean Petri slides in the dark and at −20 °C until analyses to prevent losses, photochemical reactions and biological processes. The entire set of collected samples covers most of the year (total 2190). The quantification of the water soluble inorganic ions was limited to a subset of 60 samples per site (total 360) collected in 6 periods of 10 consecutive days in the middle of April, June, August, October, December and February. Periods were chosen to be representative of all the seasons and include the dates when home heating was switched off (15 April) and on (15 October) as established by the national legislation. A ~2 cm^2-wide subsample of each filter was extracted in vials with 10 mL MilliQ water (resistivity= 18.2 MΩ·cm at 25°C, Millipore) and sonicated for 50 min. Vials were capped to avoid artifacts and sample evaporation. Extracts were pre-filtered on microporous (0.45 µm) PTFE membranes and injected in two Metrohm (Switzerland) ion chromatographic systems with conductivity detectors to quantify the concentrations of five anions (F^-, Cl^-, NO_3^-, PO_4^{3-}, SO_4^{2-}) and five cations (Na^+, NH_4^+, K^+, Mg^{2+}, Ca^{2+}). Anions were separated on a Metrosep A Supp 7–250/4.0 column applying a isocratic flow (0.8 mL min^{-1}) of 360 mM Na_2CO_3 (Sigma-Aldrich, ACS ≥99.8%) eluent. Cations were determined using a Metrosep C 3–150/4.0 column and a 1 mL min^{-1} isocratic flow of 3 mM ultrapure HNO_3 (Fluka, TraceSELECT, ≥69%). Single-ionic standards were prepared from pure salts and used to test the linearity and calibrate the instrumental responses. The analyses were routinely checked by using certified liquid standards (Fluka, TraceCERT) diluted in MilliQ water. The relative repeatability of each ion determination (standard deviation of 10 replications) was <5%. Field

blanks were prepared and analysed together with the samples and the values obtained were routinely subtracted. Limits of detections (LODs) were calculated as three times the standard deviation of field blanks: data below the LODs were substituted by LOD/2.

Other chemical parameters were automatically determined on hourly or bihourly basis in each site following European standards: NO, NO_2, NO_x (EN 14211:2012); SO_2 (EN 14212:2012); O_3 (EN 14625:2012); PM_{10} and $PM_{2.5}$ with automatic beta-attenuation monitor systems. A comprehensive list of measured parameters in each site is provided in Table 1.

2.3 Sampling Artifacts

A number of studies have reported that potential artifacts can occur during air sampling because of ambient conditions and the interactions between collected particles and gaseous compounds with each other or with the filter medium (e.g., Appel et al., 1984; Dasch et al., 1989; Harrison et al., 1990; Harrison and Kitto, 1990; Koutrakis et al., 1992; Zhang and McMurry, 1992; Cheng and Tsai, 1997; Pathak et al., 2004a; Schaap et al., 2004a; Pathak and Chan, 2005). Generally, the most evident artifact is the evaporation of nitrate due to its gas-particle partitioning (negative artifact), which is further enhanced by higher temperatures and drier air. Also, pressure drop across the filter and mixing of acidic and alkaline particles on the filter may perturb the gas-particle equilibrium. On the contrary, absorption of gas-phase nitric acid may also occur (positive artifact) mainly driven by the presence of sea-salt particles.

Studies conducted in the Po Valley (Putaud et al., 2002; Schaap et al., 2004a) have reported that nitrate volatilization generally dominates over absorption. In particular, Schaap et al., (2004a) concluded that quartz filters have a full retention of nitrate at temperatures <20°C. In

this study, all the samplers were installed into air conditioned cabins with an internal constant temperature below 20°C. Subsequent filter transport, handling and analysis were carried out under the same controlled conditions, while filter storage was at −20 °C. Moreover, the prevailing high relative humidity recorded at all of the sites (average >70% RH) during the sampling periods further decreased the potential nitrate loss. For these reasons, negative artifacts of nitrate can be considered negligible. Positive artifacts are also expected to be small: concentrations of Na^+ and Cl^- (as tracers of sea-salt) and Mg^{2+} and Ca^{2+} (as tracers of crustal particles) during the study were very low.

Another potential positive artefact can be caused by the absorption of SO_2 on collected particles, which can be subsequently oxidized to sulphate (Pathak and Chan, 2005). Due to the very low concentrations of SO_2 in Veneto (ARPAV, 2013) and according to data obtained with and without the use of denuders by Vecchi et al. (2009), sulphate can be considered a conserved specie in the Po Valley (i.e. not subject to adsorption or volatilisation).

In summary, sampling conditions and chemical results indicate that potential artifacts in this study are small. For this reason, all the chemometric analyses have been performed on raw data.

2.4 Back-Trajectory and CWT Analysis

Back-trajectories were computed to study the history of air masses during the sampling days. Set-up: HYSPLIT model (Draxler and Rolph, 2013; Rolph, 2013); 96 h backward; starting height at 20 m a.s.l.; 4 trajectories per day at 3, 9, 15 and 21 UTC calculated separately for all the sites. A clustering algorithm using the Euclidean distance measure (Carslaw, 2014) was

applied to gain information on pollutant species with similar chemical histories by grouping back-trajectories into clusters depending on their potential origin.

CWT is a back-trajectory-based hybrid receptor model used to assess potential source areas affecting air pollution at a receptor site. Briefly, each grid cell *ij* in a grid domain was used to compute the weighted concentration obtained by averaging sample concentrations that have associated trajectories passing the grid cell according to:

$$C_{ij} = \frac{1}{\sum_{k=1}^{N} \tau_{ijk}} \sum_{k=1}^{N} (C_k)\tau_{ijk}$$

where *i* and *j* are the coordinates of grid, *k* the trajectory index, *N* the number of trajectories, C_k the pollutant concentration measured at the receptor site upon arrival of the trajectory *k*, and τ_{ijk} represents the residence time of trajectory *k* in the *ij* cell. Further insights are provided in Seibert et al. (1994) and Hsu et al. (2003). Cluster analysis and CWT were computed using R and the 'Openair' package (Carslaw and Ropkins, 2012; Carslaw, 2013).

3. RESULTS

3.1 Overview of Results

Table 2 summarises the annual average concentrations of $PM_{2.5}$ and ions and also gives statistics for SIA (as sum of ammonium, nitrate and sulphate) and ΣWSII (sum of all the analysed water soluble inorganic ions). Due to the high percentage of samples below the LODs, F^-, Mg^{2+} and PO_4^{3-} were excluded from the statistics. A comprehensive list of results for each month is provided as Supplementary Information Table SI1. The $PM_{2.5}$ annual average concentrations (365 days) ranged from a minimum of 16 μg m^{-3} in BL and a maximum of 28 μg m^{-3} in PD. In the study period, the European annual average target value of 25 μg m^{-3} (2008/50/EC Directive) was breached in three sites (PD, RO, VI). On an annual

basis, ΣWSII accounted for a significant fraction of the total $PM_{2.5}$ mass, ranging from 30% (BL) to 41% (RO) and generally showed a slightly increasing trend from north to south. Annually, the most abundant ion in all the sites (Figure 1b) was nitrate, ranging from 36% (BL) and 47% (VI) of the ΣWSII, followed by sulphate 22% (VI)−29% (BL, VE), ammonium 17% (BL, TV)−21% (VI, RO) and potassium 3% (RO, VI)−5% (BL). Sodium varied from 1% (VI) and 5% (TV), while the remaining single ions never exceeded 2%. The annual levels of $PM_{2.5}$ and $PM_{2.5}$-bound nitrate, sulphate and ammonium in this study are very similar to those recorded in other urban sites in the Po Valley (Table SI2).

Gaseous pollutants were recorded for all the year on hourly basis and data were averaged to give daily mean values (Table 2 and Table SI1). The annual average concentrations of NO during the selected periods varied from 12 µg m^{-3} (TV) to 27 µg m^{-3} (PD); NO_2 from 23 µg m^{-3} (BL) to 37 µg m^{-3} (PD and RO); NO_x from 45 µg m^{-3} (BL and TV) to 79 µg m^{-3} (PD); O_3 from 46 µg m^{-3} (RO) to 61 µg m^{-3} (PD); SO_2 from 1 µg m^{-3} (PD) to 2.8 µg m^{-3} (VE). These mean concentrations are very close to the annual average levels and demonstrate that the selected periods are representative of the annual concentrations.

The annual average NO_2 levels never exceeded the Limit Value fixed by the European Directives (40 µg m^{-3}). In Veneto the emission inventory (EI) for 2007/8 (ARPAV and Regione Veneto, 2013) reported that road transport was the main source of NO_x (52111 Mg y^{-1}), followed by combustion in manufacturing industry (15119 Mg y^{-1}), other mobile sources and machinery (13793 Mg y^{-1}), combustion in energy and transformation industries (7322 Mg y^{-1}) and non-industrial combustion plants (7187 Mg y^{-1}), while remaining EMEP/EEA sources (production processes, agriculture, waste treatment and disposal, solvent and other product use, extraction and distribution of fossil fuels and geothermal energy and

312 other sources and sinks) accounted for 3216 Mg y^{-1}. The annual average levels of SO_2 were
313 very low at all the sites and well below the European limit value. The EI reported that in
314 2007/8 the main contributors in Veneto were (in Mg y^{-1}): combustion in energy and
315 transformation industries (5077)> combustion in manufacturing industry (4578)> other
316 mobile sources and machinery (2340)> production processes (1879)> non-industrial
317 combustion plants (1327)> sum of other EMEP/EEA sources (165).
318
319 It should be noted that most of the NO_x was emitted at ground level by mobile sources,
320 whereas most of SO_2 emissions originated from stationary sources via chimneys. SO_2 may
321 disperse widely from elevated sources, but the NO_x sources are themselves widely
322 distributed.
323
324 **3.2 Seasonal Variations**
325 The $PM_{2.5}$ time series are reported as Supplementary Information Figure SI1 and exhibit
326 seasonal trends at all of the sites, i.e. higher levels during winter and lower in summer, as
327 commonly observed in most sites in the Po Valley (e.g., Marcazzan et al., 2003; Vecchi et al.,
328 2004; Perrone et al., 2012; Tositti et al., 2014). The seasonality is strongly linked to weather
329 conditions, such as prolonged atmospheric stability, shallower mixing layers, wind calm
330 periods and low temperatures, which favor the accumulation of atmospheric pollutants at the
331 ground level (Ferrero et al., 2010). The increased use of wood for domestic heating in winter
332 and the burning of biomass such as straw and crop residues in the harvest season (late
333 autumn) may also have a role in raising the $PM_{2.5}$ levels. The semi-volatility of ammonium
334 nitrate may also be important. The time series also showed a number of single peaks of
335 concentration at various sites. In most cases these peaks occurred at individual sites and were
336 therefore linked to local and occasional phenomena. However, it is evident that the highest

337 concentrations were recorded on January 6th for all stations except BL, when thousands of
338 folk fires of wooden material were lit in most of the Veneto region for a local religious
339 celebration. This episode was extensively reported by Masiol et al. (2014b) and recorded
340 extremely high daily concentrations of $PM_{2.5}$, ranging from 136 μg m^{-3} in VI to 202 μg m^{-3} in
341 RO. This period was not included in the present study.
342
343 On a monthly basis, each ion exhibited a typical seasonality and similar seasonal trends were
344 generally observed in all the territory. Figure 2 reports the mass concentration time series of
345 the three SIA components, while seasonal average levels for all ions are shown as Figure SI2.
346 Results for SIA ions show that both the concentrations and the daily variations of SIA at the
347 four sites in the flatter areas of the Po Valley (VI, VE, PD and RO) are quite similar and are
348 in line with results observed at urban sites in other nearby regions (Table SI2). Low SIA
349 concentrations were recorded at all sites in June, and in October in the Alpine valley (BL),
350 the SIA components were extremely low as well. Nitrate concentrations in PM are inversely
351 related to the ambient temperature: they are higher in the colder months, mainly because
352 ammonium nitrate tends to volatilise at temperatures above 20°C (Schaap et al., 2004a;
353 Vecchi et al., 2009). This is observed all over Europe (e.g., Allen et al., 1989; Schaap et al.,
354 2004b; Revuelta et al., 2012). Sulphate presents a peculiar bimodal seasonality, with two
355 maxima in August and February. A peak in the warmest period is commonly recorded in
356 Europe (e.g., Revuelta et al., 2012) and is probably due to the increased photochemical
357 activity favouring the oxidation of SO_2 via hydroxyl radical reaction (Stockwell and Calvert,
358 1983; Khoder, 2002; Seinfeld and Pandis, 2006), whereas the peak in February may be
359 associated with aqueous phase oxidation. Ammonium concentrations tend to parallel those of
360 nitrate and sulphate. Calcium shows no evident seasonality. However slightly higher levels
361 were recorded in August and winter. Potassium, a known tracer of biomass combustions,

(e.g., Puxbaum et al., 2007; Saarnio et al., 2010) presents an evident seasonality with higher concentrations in the coldest period. Wood (i.e. logs, briquettes, chips and pellet) is becoming a popular renewable alternative to natural gas in Northern Italy (Pastorello et al., 2011) and the increasing emissions from its use for domestic heating can be considered the most plausible source. Chloride has a seasonal behavior similar to potassium. Its presence in PM can derive from various sources, i.e. sea-salt, biomass burning, resuspension of road deicing salts, coal combustion and various industrial processes. The marine origin can be probably excluded as no significant gradients of concentration are observed from the stations close to the coast (VE) to the more continental ones (VI and PD). Therefore, biomass burning and the resuspension of road salt are probably the most important sources.

Seasonal trends of gaseous pollutants are also given in Figure SI2. Nitrogen oxides increased during the cold season due to changes in mixing depths and emission rates, while ozone reached the highest levels in the warmest period due to its photochemistry. Sulfur dioxide showed no clear seasonal trends, but reached the highest levels in VE during the warmest period (June-August).

3.3 Spatial Variations

Starting from the evidence that $PM_{2.5}$ and most ions have quite similar seasonal trends at all the sites, an inter-site comparison of the annual concentrations was conducted for each ion. Since the data were not distributed normally, the nonparametric Kruskal–Wallis one-way analysis of variance was used. This test is based on the rank of each sample instead of its value and the null hypothesis assumes that the central values of the groups (medians) are equal, and is rejected for $p< 0.05$. Thus, the post hoc Dunn's test was applied to identify which sites are significantly different from the others. Results generally show that $PM_{2.5}$, nitrate, sulphate and ammonium in BL and TV are significantly ($p<0.05$) different from the

387 other sites and concentrations increased from North (mountain) to South (lowland) and from
388 East (coastal) to West (more continental). On the other hand, K^+ and Ca^{2+} levels are not
389 significantly different and their concentrations are therefore uniform in all of the Veneto
390 region. These results show that biomass burning, which has been identified as a major source
391 of potassium, and the re-suspension of mineral dust and soil, which is the major source of
392 calcium, are quasi-uniformly distributed throughout the region.
393
394 An indirect quantification of differences in concentrations among the sites was carried out by
395 regressing $PM_{2.5}$ mass concentration and nitrate+sulphate (expressed as neq m^{-3}) among
396 pairs of sites (intercept forced to zero). Results are provided in Figures SI3 and SI4,
397 respectively. Results for both $PM_{2.5}$ and nitrate+sulphate show that sites located in the main
398 Po Valley (VI, VE, PD and RO) have regression slopes around 1 (0.84—1.17) and high
399 coefficients of determination (R^2>0.8), which indicate good agreement between
400 concentrations. On the contrary, slopes (range 1.26—1.42) and R^2 (≤0.2) between BL and
401 sites in the main Po Valley indicate a very poor agreement. TV has an intermediate behavior
402 with sites in the main Po Valley: it presents a moderate relationship (R^2 0.6—0.8), but high
403 slopes (1.2—1.8).
404
405 The spatial and temporal relationships among the sites for $PM_{2.5}$ and ionic species were
406 further investigated by using correlation analysis. A preliminary inter-site correlation analysis
407 among the $PM_{2.5}$ concentrations for the whole year (365 days) was conducted. The $PM_{2.5}$
408 distributions were tested for normality by applying the Shapiro-Wilk's tests and the normality
409 assumption at p< 0.05 was not met. A Box-Cox transformation of the dataset was therefore
410 made. The resultant transformed data were normally distributed and Pearson's correlation
411 analysis was run. Results (Table 3) generally show significant correlations (p<0.01, r>0.8)

among all the sites, with the exception of BL, which appears slightly less correlated (r≈0.7) with the others. $PM_{2.5}$ exhibits a similar temporal trend in all the cities even if these are located in different territories of the region. It is evident that the processes of emission, accumulation and removal are quite similar in the six cities.

However, the correlation analysis for the full dataset may be affected by the marked seasonality of the variables, with the result that the correlation links variables with similar seasonal trends and not sites with simultaneous daily variations. This problem was solved by monthly-averaging the original data: the monthly means were subtracted from each daily value in each selected period. This normalisation procedure had also the advantage of generating variables that were quasi-normally distributed. The correlation matrices of the monthly-averaged data are reported in Table 3 and show that the $PM_{2.5}$ is still strongly correlated at all the sites located in the lowland area, while the mountain site (BL) is less correlated. Sulphate has usually significantly ($p< 0.05$) positive relationships for all pairs of sites, indicating that it has a similar (synchronous) behavior in the whole region. Highly (r> 0.75) significant correlations are also found for $PM_{2.5}$, nitrate and ammonium, except at BL which appears to be uncorrelated with the other sites. Potassium is very well correlated in the central part of the region (VI, VE, PD), while significant but weak correlations are found in TV and RO, and BL is uncorrelated with the other sites. Calcium shows few inter-site correlations (Table SI3).

This analysis generally shows that $PM_{2.5}$, potassium, nitrate, sulphate and ammonium follow a similar day-to-day trend at all sites throughout the region, in particular in the lowland territory, and confirms that both the emission sources and the accumulation/removal

processes in the region are similar. A similar finding was also recently reported for the levels of PM_{10}-bound polycyclic aromatic hydrocarbons at 21 sites in Veneto (Masiol et al., 2013).

4. DISCUSSION

The SIA mass is generally calculated as the simple sum of ammonium, sulphate and nitrate or is derived from the results of source apportionment approaches. Nevertheless, its prediction is not straightforward because the ion generation, transport, aging or removal in the particle-phase strongly depends on weather conditions, but also on the presence of precursor gases and oxidant species (mainly hydroxyl radical, hydrogen peroxide and ozone). Basically, SIA generation is a two-step process, in which the gaseous precursors SO_2 and NO_x undergo photochemical and heterogeneous thermal oxidation to form sulfuric and nitric acids, respectively. Subsequently, the acids are neutralised by ammonia, and in the case of ammonium nitrate, partitioned according to thermodynamic equilibria, mostly determined by temperature and relative humidity (Baek et al., 2004; Seinfeld and Pandis, 2006; Allen et al., 1989). Reactions with other ions may also form mixed salts. Using the experimental data obtained in this study, some preliminary conclusions regarding the SIA are drawn.

4.1 Sulfur and Nitrogen Oxidation Ratios

The degree of atmospheric conversion of gaseous precursors, SO_2 and NO_2, to sulphate and nitrate, respectively, can be indirectly assessed by means of the sulfur (SOR) and nitrogen (NOR) oxidation ratios:

$$\mathrm{SOR} = \frac{\mathrm{n\text{-}nss}SO_4^{2-}}{\mathrm{n\text{-}nss}SO_4^{2-} + \mathrm{n}SO_2}$$

$$\mathrm{NOR} = \frac{\mathrm{n\text{-}}NO_3^-}{\mathrm{n\text{-}}NO_3^- + \mathrm{n}NO_2}$$

where the n units are in moles m^{-3} and nss-SO_4^{2} is the non-sea-salt sulphate calculated as $[SO_4^{2-}]- 0.25\cdot[Na^{+}]$. The SOR and NOR have been used by many authors (e.g., Khoder, 2002; Bencs et al., 2008; Behera and Sharma, 2010) to describe the degree of ageing of the air mass. The results appear as Table SI4, alongside those of other similar studies for comparison. Annually, the average SOR varied from 0.4 (VE) to 0.6 (PD) suggesting a high degree of oxidation of SO_2 in the atmosphere, while the annual average NOR ranged between 0.04 (BL) and 0.1 (PD). SOR shows no clear spatial variation and generally its seasonal concentrations follow those of sulphate. However, it is important to point out that the minimum SOR is reached at VE in the warmest period. This is probably due to the highest concentrations of SO_2 in summer caused by: (1) the peak of energy production of a coal-fired power plant meeting the demand for air conditioning; (2) the presence of higher shipping traffic using the cruise harbour. This assumption is also supported by the emission inventory for 2010 (ISPRA, 2014) showing that the Venice province has the highest production of SO_2 (4586 Mg y^{-1}), followed by Padova (1324 Mg y^{-1}). About 71% of the emissions in VE are attributed to combustion in energy and transformation industries. Spatially, NOR seems to increase slightly from North to South and from the coast to the mainland.

4.2 Ammonia Availability and Neutralisation Ratio

Ammonia is known to neutralise sulfuric acid irreversibly, and then nitric acid. In addition, hydrochloric acid may react with gaseous ammonia to form ammonium chloride aerosol. However, in thermodynamic equilibrium conditions ammonium chloride is reported to be 2-3 times more volatile than ammonium nitrate (Stelson and Seinfeld, 1982; Pio et al., 1992) and its formation occurs later. It is well known that in low ammonia conditions, NH_3 acts as the main limiting factor for SIA generation (Erisman and Schaap, 2004). On the other hand, in case of high NH_3 availability, ammonium nitrate formation is principally limited by the

availability of nitric acid. These conditions are important in agricultural areas because livestock farming and the use of soil fertilizers are primary sources of atmospheric NH_3 (Galloway et al., 2004; Sutton et al., 2008). Recent modeling simulations on a continental scale (Wichink Kruit et al., 2012) have reported that ammonia levels in the Po Valley are among the highest in Europe (range 4−10 μg m^{-3}). This is also confirmed by satellite observations (Clarisse et al., 2009) indicating the Po valley as one of the most evident hotspots for NH_3 at a global scale. The 2010 Italian emission inventories (ISPRA, 2014) reported that ~$50.2 \cdot 10^3$ Mg of NH_3 are emitted annually in Veneto, most of which is from agriculture ($48.9 \cdot 10^3$ Mg), followed by road transport ($0.7 \cdot 10^3$ Mg). Because SO_2 emissions have been sharply reduced in the last decades in most developed countries, including Italy (Manktelow et al., 2007; Hamed et al., 2010), more NH_3 is available for the formation of ammonium nitrate (Bauer et al., 2007; Pye et al., 2009). Recent data indicated that in Veneto SO_2 concentrations are generally < 8 μg m^{-3}, i.e. below the EU lower threshold (ARPAV, 2013).

Reactions of gaseous acids with other particles (e.g., sea salt, crustal dust, anthropogenic) can form secondary salts, mainly replacing Cl^- with sulphate and nitrate, or forming salts with Na^+, K^+, Mg^{2+} or Ca^{2+}. For example, sulphate and nitrate may affect the hygroscopic behaviour of mineral dust (Shi et al., 2008) and may form nitrate-containing particles mainly in the coarse mode (Pakkanen et al., 1996; Metzger et al., 2006).

However, in this study, the masses of Na^+, Mg^{2+}, Ca^{2+} and Cl^- were low, if compared to NH_4^+, NO_3^- and SO_4^{2-} and therefore their contribution to salts in $PM_{2.5}$ can be assumed to be negligible. From a linear regression analysis between ammonium and the sum of nitrate and sulphate (expressed as neq m^{-3}) significant coefficients of determination (R^2 varying from

507 0.94 in BL and 0.99 in VI, VE and RO), almost unitary slopes (from 0.83 in BL 1.06 in VI,
508 VE and RO) and very low intercepts were obtained for all the sites. The scatterplots are
509 reported as Figure SI5. They also reveal that the relationships are constantly linear in all the
510 seasons, even if the mass contributions of each ion varied greatly during the year.
511
512 The neutralisation ratio (NR) (Bencs et al., 2008), also called acidity ratio (Engelhart et al.,
513 2011), expresses the degree of neutralisation of sulphate and nitrate by ammonium
514 (concentrations are in equivalents) and was used to describe the aerosol acidity:

$$\mathrm{NR} = \frac{[\mathrm{NH_4^+}]}{[\mathrm{SO_4^{2-}}] + [\mathrm{NO_3^-}]}$$

515 Figure 3 shows the NR time series and permits some inferences: (i) on an annual basis,
516 average NRs were equal to 1 within the analytical variability, or slightly less: 0.8 in BL, TV,
517 PD and 0.9 in VI, VE, RO; (ii) the lowest NRs were recorded in spring, while they were
518 almost constant in the remaining months at all the sites; (iii) both the concentrations and the
519 daily variations of SIA at the 4 sites in the Po valley had similar trends; (iv) NR variability in
520 August and February, i.e. in the warmest and coldest months of the year, respectively, was
521 small, while strong daily changes were recorded in April and October. It is unclear if this
522 trend is linked mainly to a discontinuity of the sources (e.g., domestic heating switching off
523 and on), to weather factors controlling the SIA generation, or to external transport effects.
524
525 To investigate the extent of neutralisation of the SIA in more detail, NR was plotted against
526 the ammonium concentration (Figure 4a). Results show that for all the sites: when
527 concentrations of NH_4^+ exceed ~150 neq m^{-3}, the NR appears to be constant around 1 and
528 SIA is likely to be composed of ammonium nitrate and ammonium sulphates; for lower levels
529 of ammonia, the variability of NR increases and, generally, the ratio becomes smaller. These

results confirm that ammonia may effectively act as a limiting agent for SIA and suggest that during ammonia-limiting conditions, sulfuric and nitric acids may react with other particles to form salts. This assumption can be further confirmed by plotting the NR versus ionic balance (ratio between the sum of all analysed cations and anions) (Figure 4b). The graph clearly shows that most of samples are set in the 4^{th} quadrant, a region where the relative lack of ammonium (NR<1) corresponds to an excess of cations (cations>anions), i.e. nitrate and sulphate are potentially combined with other cations than ammonium. Figure 4b also shows that no samples are plotted in the opposite quadrant (2^{nd}), demonstrating that on days with an excess of ammonium (NR>1) no excess anions are present, thus showing the absence of other inorganic salts of ammonium, such as NH_4Cl. A few samples mainly pertaining to the mountain site (BL) are scattered in the 1^{st} and 3^{rd} quadrants: samples in the 1^{st} quadrant are characterised by an excess of ammonium and a positive ionic balance, i.e. an excess of positive charges probably neutralised by organic acids, not measured in this study. Samples in the 3^{rd} quadrant were almost all collected in April and a possible explanation is that the lack of positive charges may be balanced by H^+ (which was not measured), resulting in acid aerosol.

4.3 Potential Contribution of Long-Range Transport

The analysis of the back-trajectories was used to give some insight into the potential contribution of long-range aerosol transport upon the Veneto region. As known from the literature, the use of trajectories has some limitations in accuracy for various reasons (e.g., Stohl et al., 1998). However, taking into account the range of associated uncertainties, the use of some trajectory statistical methods is recognised as very useful to investigate potential source areas (Kabashnikov et al., 2011; Abdalmogith and Harrison, 2005).

554 For the purpose of this study, the variability of back-trajectories was tested using different
555 starting heights and hours: errors associated with a single trajectory were reduced by
556 simulating four trajectories for each sampling day (at 6, 12, 18, 24 local time). The cluster
557 analysis was applied to all the 4-days back-trajectories computed and for the each site, i.e. 4
558 trajectories every day, which have been merged with daily data. In fact, this expedient
559 allowed the spread of daily chemical data over 4 trajectories and thus can account for days
560 that may have changes in trajectories within 24-h. The number of extracted clusters was
561 carefully evaluated by analysing the change in the total spatial variance and the best
562 compromise was 5 clusters for all the sites. Results show that all sites present similar mean
563 trajectories (Figure 5) named (1) Western Europe, (2) Mediterranean, (3) local, (4) Northern
564 Europe and (5) Eastern Europe. Statistics for chemical composition data in each cluster are
565 presented as boxplots in Figures 5 and SI6. The number of trajectories grouped in each
566 cluster generally differ among BL, TV and other sites (Table SI5). The reason is linked to the
567 topography of the territory: BL is located in an alpine valley, TV is at the border of Alps,
568 whereas other sites are located in flatter areas of the Po Valley. As a consequence, results for
569 BL and TV differ from the other sites with results sometimes showing opposite trends.
570 Generally, $PM_{2.5}$, nitrate and K^+ show similar results, with concentrations higher for cluster 3
571 in BL and TV and for clusters 1, 4 and 5 for the remaining sites. Sulphate in BL and TV
572 appears to have higher concentrations when air masses are associated with clusters 1 and 5,
573 whereas it is associated with clusters 3 and 5 at the other sites. Calcium and chloride show
574 only small differences. Sites BL and TV show a different behaviour with respect to $PM_{2.5}$.
575 The highest concentrations are associated with trajectory 3, which for the other sites shows
576 the lowest $PM_{2.5}$. This effect is probably the result of trapping of lower level emissions at BL
577 and TV in the slow moving northerly air. With regard to high sulphate and nitrates, these
578 sites behave rather similarly to the others as a results of regional influences.

On the other hand, the analysis of the potential effects of long-range transport on a regional scale through the CWT model returned very similar results at all sites and clearly indicate some predominant source areas for potential transboundary transport of $PM_{2.5}$ and some ions (Figures 6a and 6b). In particular, a wide area spanning across Eastern and Central Europe and Northern Italy is identified as a main potential source of all species. Similar results have also been obtained from a previous study conducted at a site near VE during 2009-2010 (Squizzato et al., 2014). In addition, other minor source areas are also identified: an area in Central Italy which roughly coincides with the heavily populated areas of Rome and Naples as a source of $PM_{2.5}$ nitrate, and an area in North Africa, which may be linked to Saharan dust outbreaks. CWT also shows that air masses passing over continental Europe are responsible for the highest NR and SOR, while this effect is less evident for NOR (Figure SI7). If NR, SOR and NOR are taken as indicative of the aging of air masses (generally highest values of oxidation ratios and NR values close to 1 are expected in aged air masses) these results stress that transboundary transport from continental Europe may have an important impact on levels of secondary species in the Po Valley. The lower values of NOR than SOR probably reflect the higher local emissions of NO_x compared to SO_2.

4.4 Analysis of Single Episodes

Three episodes of high SIA concentrations occurred during the campaign (Figure 2): (1) 15th to 21st October, (2) 13th to 17th February and (3) 17th to 22nd February. Despite all sites showed covariant daily variations in the levels of nitrate, some differences during those episodes were identified. A further analysis of single back-trajectories was thus performed to explain why some sites are generally experiencing much lower concentrations than others. Figure 7 shows the single back-trajectories associated with the daily concentration of SIA. In

the first and third episodes, it is evident that all sites show similar daily air mass pathways from the Mediterranean and Central Europe, respectively. However, only VI, VE, PD and RO show similar daily variations and levels associated with single trajectories, whereas TV had a similar daily variation, but significantly lower concentrations. There will be a number of reasons explaining this result: (i) data indicate that transboundary transport of polluted air masses may have a higher impact over the Eastern Po Valley; (ii) the cluster and CWT analyses both indicate Central Europe as a major source area of ammonium nitrate aerosol; (iii) results suggest the topography may influence the local impact of long-range transport: a general homogeneity in the SIA levels is often recorded in the flat area of the valley, while the Alpine chain may act as a barrier for the dispersion of pollutants at ground-level.

The results for the second episode are quite different. Despite all sites show similar air mass histories, the levels of SIA were higher in RO and VI. As the differences cannot be explained by differing air mass origins, it can be concluded that ammonium nitrate generation may also occur locally as a consequence of oxidation of locally emitted NO_x.

In conclusion, these results indicate that SIA pollution may be sensitive to both long-range transport and local generation processes. Due to the relatively short period investigated in this study (60 days over one year), there is a limit to the conclusions which may be drawn. However, as a few events such as those considered in detail can have a considerable effect upon the annual mean $PM_{2.5}$ concentration, the different characteristics and effects of long-range or local SIA episodes should be investigated in more detail over a longer period, by collecting a large number of samples.

5. CONCLUSIONS

This study is the first one investigating the spatial and temporal properties of secondary inorganic aerosol in a large area of the Po Valley using simultaneous experimental measurements at multiple receptor-sites. The statistical processing of the data shows that $PM_{2.5}$ and individual ions to have very similar concentrations across all urban sites and to be very well correlated throughout the region, even though the sampling stations are located in different cities and in an area ~$18.4 \cdot 10^3$ km^2-wide. Therefore, it can be concluded that the PM pollution and the relative amount of SIA in the Veneto is quasi-uniformly distributed throughout the region and the formation and removal processes affecting all sites are quite similar. Moreover, a comparison with previous studies conducted in other nearby regions of NE Italy indicates quite constant levels, seasonal trends and speciation of SIA over a wide area of the Po Valley. The main results can be summarised as follows:

- Annually, water soluble inorganic ions account from 30% to 41% of the total $PM_{2.5}$ mass concentrations and the most abundant ion is nitrate (36%−47%), followed by sulphate (22%−29%), ammonium (17%−21%) and potassium (3%−5%).
- Each ion exhibits a characteristic seasonality and similar seasonal trends are generally recorded over the entire study area.
- $PM_{2.5}$, nitrate, sulphate and ammonium in BL and TV are significantly different from other sites and generally levels of analysed pollutants increased from North (mountain) to South (lowland) and from East (coastal) to West (more continental). In contrast, K^+ and Ca^{2+} show weak spatial gradients.
- Potassium, nitrate, sulphate and ammonium also show similar daily trends throughout the region, in particular in the lowland territory, and confirm that both the sources and the accumulation/removal processes in the region are similar.

- The neutralisation ratio and the ionic balance were jointly investigated to provide information about the processes affecting SIA and the interactions between the secondary ions and other particles. Results confirm the probable formation of secondary salts with potassium, sodium and calcium.
- The application of trajectory-based methods (cluster and CWT analyses) was useful to identify potential source areas leading to increases in $PM_{2.5}$ and ions concentrations across the region. Results showed that higher concentrations of all analysed species are mainly associated with air masses originating in a widespread area located in the Eastern-Central Europe. Central Italy and Northern Africa are also identified as possible source areas particularly for $PM_{2.5}$ and K^+.
- The analysis of three single episodes of high ammonium nitrate levels indicate that both long-range transport and local formation processes may lead to high SIA levels during colder months. Those events have a large potential for raising the annual average levels of $PM_{2.5}$ and should be investigated in more detail.

As a final remark, this study concluded that SIA pollution has similar and concurrent effects over the entire study area and probably in the whole Po Valley. Findings clearly indicate that any action to mitigate the $PM_{2.5}$ pollution to meet the present target and the future air quality standards in Veneto must be taken concurrently in the entire region and well beyond its boundaries.

ACKNOWLEDGEMENTS

This study was conducted within an agreement between the Ca' Foscari University of Venice and ARPAV. The authors gratefully acknowledge the NOAA Air Resources Laboratory

(ARL) for the provision of the HYSPLIT transport and dispersion model and/or READY website (http://www.ready.noaa.gov) used in this publication.

DISCLAIMER

This study was not financially supported by any public or private institution. We would like to stress that the views expressed in this study are exclusively of the authors and do not necessarily correspond to those of ARPAV.

REFERENCES

Abdalmogith S.S., Harrison R.M., 2005. The use of trajectory cluster analysis to examine the long-range transport of secondary inorganic aerosol in the UK. Atmospheric Environment 39, 6686-6695.

Allen, A. G., Harrison, R.M., Erisman, J. W., 1989. Field measurements of the dissociation of ammonium nitrate and ammonium chloride aerosols. Atmospheric Environment 23, 1591-1599.

Andreani-Aksoyoglu, S., Prévôt, A. S. H., Baltensperger, U., Keller, J., Dommen, J., 2004. Modeling of formation and distribution of secondary aerosols in the Milan area (Italy). Journal of Geophysical Research 109 (D5), D05306. doi:10.1029/2003JD004231.

Appel, B.R., Tokiwa, Y., Haik, M., Kothny, E.L., 1984. Artifact of particulate sulfate and nitrate formation on filter media, Atmospheric Environment 18, 409–416.

ARPAV (Environmental Protection Agency of Veneto Region), 2013. Regional Report of Air Quality–Year 2012, pp. 85 [in Italian]. Available at: http://www.arpa.veneto.it/temi-ambientali/aria/riferimenti/documenti

Baek B. H., Aneja V. P., Tong Q., 2004. Chemical coupling between ammonia, acid gases, and fine particles. Environmental Pollution 129, 89–98.

Bauer, S. E., Koch, D., Unger, N., Metzger, S. M., Shindell, D. T., Streets, D. G., 2007. Nitrate aerosols today and in 2030: a global simulation including aerosols and tropospheric ozone. Atmospheric Chemistry and Physics 7, 5043-5059.

Behera S. N., Sharma M., 2010. Investigating the potential role of ammonia in ion chemistry of fine particulate matter formation for an urban environment. Science of the Total Environment 408, 3569-3575

Bencs, L., Ravindra, K., de Hoog, J., Rasoazanany, E. O., Deutsch, F., Bleux, N., Berghmans, P., Roekens, E., Krata, A., Van Grieken, R., 2008. Mass and ionic composition of atmospheric fine particles over Belgium and their relation with gaseous air pollutant. Journal of Environmental Monitoring 10, 1148–1157.

Benson D. R., Yu J. H., Markovich A., Lee S.-H., 2011. Ternary homogeneous nucleation of H2SO4, NH3, and H2O under conditions relevant to the lower troposphere. Atmospheric Chemistry and Physics 11, 4755-4766.

Carslaw D. C., Ropkins K., 2012. openair - an R package for air quality data analysis. Environmental Modelling & Software 27-28, 52-61.

Carslaw D. C., 2014. The openair manual — open-source tools for analysing air pollution data. Version 10th June 2014, King's College London.

Cheng, Y.H. Tsai, C.J., 1997. Evaporation loss of ammonium nitrate particles during filter sampling. Journal of Aerosol Science 28, 1553–1567.

737 Clarisse, L., Clerbaux, C., Dentener, F., Hurtmans, D., Coheur, P. F., 2009. Global ammonia
738 distribution derived from infrared satellite observations. Nature Geoscience 2, 479-483.
739
740 Dasch, J.M., Cadle, S.H., Kennedy, K.G., Mulawa, P.A., 1989. Comparison of annular
741 denuders and filter packs for atmospheric sampling. Atmospheric Environment 23, 2775–
742 2782.
743
744 Decesari, S., Allan, J., Plass-Duelmer, C., Williams, B. J., Paglione, M., Facchini, M. C.,
745 O'Dowd, C., Harrison, R. M., Gietl, J. K., Coe, H., Giulianelli, L., Gobbi, G. P., Lanconelli,
746 C., Carbone, C., Worsnop, D., Lambe A. T., Ahern, A. T., Moretti, F., Tagliavini, E., Elste,
747 T., Gilge, S., Zhang, Y., Dall'Osto, M., 2014. Measurements of the aerosol chemical
748 composition and mixing state in the Po Valley using multiple spectroscopic techniques.
749 Atmospheric Chemistry and Physics 14, 12109-12132.
750
751 de Leeuw F.A.A.M., 2002. A set of emission indicators for long-range transboundary air
752 pollution. Environmental Science and Policy 5, 135-145.
753
754 Draxler R.R., Rolph G.D., 2013. HYSPLIT (HYbrid Single-Particle Lagrangian Integrated
755 Trajectory) Model access via NOAA ARL READY Website
756 (http://www.arl.noaa.gov/HYSPLIT.php). NOAA Air Resources Laboratory, College Park,
757 MD.
758 EEA (European Environment Agency), 2013. AirBasedThe European Air Quality Database.
759 Available from: http://www.eea.europa.eu/themes/air/airbase (last accessed January, 2013).
760
761 Engelhart, G. J., Hildebrandt, L., Kostenidou, E., Mihalopoulos, N., Donahue, N. M., Pandis,
762 S. N., 2011. Water content of aged aerosol. Atmospheric Chemistry and Physics 11, 911-920.
763
764 Erisman, J.W., Schaap M., 2004. The need for ammonia abatement with respect to secondary
765 PM reductions in Europe. Environmental Pollution, 129, 159-163.
766
767 Ferrero L., Perrone M.G., Petraccone S., Sangiorgi G., Ferrini B. S., Lo Porto C., et al., 2010.
768 Vertically-resolved particle size distribution within and above the mixing layer over the
769 Milan metropolitan area. Atmospheric Chemistry and Physics 10, 3915-3932.
770
771 Galloway, J. N., Dentener, F. J., Capone, D. G., Boyer, E. W., Howarth, R. W., Seitzinger, S.
772 P., Asner, G. P., Cleveland, C. C., Green, P. A., Holland, E. A., Karl, D. M., Michaels, A. F.,
773 Porter, J. H., Townsend, A. R., Vöosmarty, C. J., 2004. Nitrogen Cycles: Past, Present, and
774 Future. Biogeochemistry 70, 153-226.
775
776 Hamed, A., Birmili, W., Joutsensaari, J., Mikkonen, S., Asmi, A., Wehner, B., G. Spindler,
777 Jaatinen, A., Wiedensohler ,A., Korhonen, H., Lehtinen, K. E. J., Laaksonen, A., 2010.
778 Changes in the production rate of secondary aerosol particles in Central Europe in view of
779 decreasing SO2 emissions between 1996 and 2006. Atmospheric Chemistry and Physics 10,
780 1071-1091.
781
782 Harrison, R.M., Sturges, W.T., Kitto, A.M.N., Li, Y., 1990. Kinetics of evaporation of
783 ammonium chloride and ammonium nitrate aerosols. Atmospheric Environment 24A, 1883–
784 1888.
785

Harrison, R.M., Kitto, A.M.N., 1990. Field intercomparison of filter pack and denuder sampling methods for reactive gaseous and particulate pollutants. Atmospheric Environment 24A, 2633–2640.

Holmes N. S., 2007. A review of particle formation events and growth in the atmosphere in the various environments and discussion of mechanistic implications. Atmospheric Environment 41, 2183–2201.

Hsu, Y. K., Holsen, T. M., Hopke, P. K., 2003. Comparison of hybrid receptor models to locate PCB sources in Chicago. Atmospheric Environment 37, 545-562.

ISPRA, 2014. Disaggregated national emission inventory 2010, Italian Institute for Environmental Protection and Research, available online: http://www.sinanet.isprambiente.it/it/sia-ispra/inventaria/versione-2.0-dell2019inventario-provinciale-delle-emissioni-in-atmosfera/view, last access: 1 September 2013.

Kabashnikov, V. P., Chaikovsky, A. P., Kucsera, T. L., Metelskaya, N. S., 2011. Estimated accuracy of three common trajectory statistical methods. Atmospheric Environment, 45, 5425-5430.

Khoder M. I., 2002. Atmospheric conversion of sulfur dioxide to particulate sulfate and nitrogen dioxide to particulate nitrate and gaseous nitric acid in an urban area. Chemosphere 49, 675-684.

Koutrakis, P., Thompson, K. M., Wolfson, J. M., Spengler, J. D., Keeler, G. J., Slater, J. L., 1992. Determination of aerosol strong acidity losses due to interactions of collected particles: Results from laboratory and field studies. Atmospheric Environment 26A, 987–995.

Manktelow, P. T., Mann, G. W., Carslaw, K. S., Spracklen, D.V., Chipperfield, M. P., 2007. Regional and global trends in sulfate aerosol since the 1980s. Geophysical Research Letter 34, L14803.

Marcazzan G. M., Ceriani M., Valli G., Vecchi R., 2003. Source apportionment of PM10 and PM2.5 in Milan (Italy) using receptor modeling. Science of The Total Environment 317, 137-147.

Masiol M., Formenton G., Pasqualetto A., Pavoni B., 2013. Seasonal trends and spatial variations of PM10-bounded polycyclic aromatic hydrocarbons in Veneto region, Northeast Italy. Atmospheric Environment 79, 811-821.

Masiol M., Squizzato S., Rampazzo G., Pavoni B., 2014a. Source apportionment of PM2.5 at multiple sites in Venice (Italy): Spatial variability and the role of weather. Atmospheric Environment 98, 78-88.

Masiol M., Formenton G., Giraldo G., Pasqualetto A., Tieppo P., Pavoni B., 2014b. The dark side of the tradition: the polluting effect of Epiphany folk fires in the eastern Po Valley (Italy). Science of the Total Environment 473-474, 549-564.

834 Metzger, S., Mihalopoulos, N., Lelieveld, J., 2006. Importance of mineral cations and
835 organics in gas-aerosol partitioning of reactive nitrogen compounds: case study based on
836 MINOS results. Atmospheric Chemistry and Physics 6, 2549-2567.
837
838 Pakkanen, T. A., Kerminen, V. M., Hillamo, R. E., Makinen, M., Makela, T., Virkkula, A.,
839 1996. Distribution of nitrate over seasalt and soil derived particles – Implications from a field
840 study. Journal of Atmospheric Chemistry 24, 189-205.
841
842 Pastorello C., Caserini S., Galante S., Dilara P., Galletti F., 2011. Importance of activity data
843 for improving the residential wood combustion emission inventory at regional level.
844 Atmospheric Environment 45, 2869-2876.
845
846 Pathak, R.K., Yao, X.H., Chan, C.K., 2004. Sampling artifacts of acidity and ionic species in
847 PM2.5. Environmental Science and Technology 38, 254–259.
848
849 Pathak, R.K. Chan, C.K., 2005. Inter-particle and gas-particle interactions in sampling
850 artifacts of PM2.5 in filter-based samplers. Atmospheric Environment 39, 1597–1607.
851
852 Perrone M. G., Larsen B. R., Ferrero L., Sangiorgi G., De Gennaro G., Udisti R., Zangrando,
853 R., Gambaro, A., Bolzacchini, E., 2012. Sources of high PM2.5 concentrations in Milan,
854 Northern Italy: Molecular marker data and CMB modeling. Science of The Total
855 Environment 414, 343-355.
856
857 Pio, C. A., Nunes, T. V., Leal, R. M., 1992. Kinetic and thermodynamic behaviour of volatile
858 ammonium compounds in industrial and marine atmospheres. Atmospheric Environment.
859 Part A. General Topics 26, 505-512.
860
861 Putaud, J.P., Van Dingenen, R., Raes, F., 2002. Submicron aerosol mass balance at urban and
862 semirural sites in the Milan area (Italy). Journal of Geophysical Research 107 (D22), 8198–
863 8208.
864
865 Putaud J.-P., van Dingenen R., Alastuey A., Bauer H., Birmili W., Cyrys J., Flentje, H.,
866 Fuzzi, S.,Gehrig, R., Hansson, H.C., Harrison, R.M., Herrmann, H., Hitzenberger, R., Hüglin,
867 C., Jones, A.M., Kasper-Giebl, A., Kiss, G., Kousa, A., Kuhlbusch, T.A.J., Löschau, G.,
868 Maenhaut, W., Molnar, A., Moreno, T., Pekkanen, J., Perrino, C., Pitz, M., Puxbaum ,H.,
869 Querol, X., Rodriguez, S., Salma, I., Schwarz, J., Smolik, J., Schneider, J., Spindler, G., ten
870 Brink, H., Tursic, J., Viana, M., Wiedensohler, A., Raes, F., 2010. A European aerosol
871 phenomenology – 3: Physical and chemical characteristics of particulate matter from 60 rural,
872 urban, and kerbside sites across Europe. Atmospheric Environment 44, 1308-1320.
873
874 Puxbaum H., Caseiro A., Sánchez-Ochoa A., Kasper-Giebl A., Claeys M., Gelencser A.,
875 Legrand, M., Preunkert, S., Pio, C., 2007. Levoglucosan levels at background sites in Europe
876 for assessing the impact of biomass combustion on the European aerosol background. Journal
877 of Geophysical Research 112, D23S05. http://dx.doi.org/10.1029/2006JD008114.
878
879 Pye, H. O. T., Liao, H., Wu, S., Mickley, L. J., Jacob, D. J., Henze, D. K., Seinfeld, J. H.,
880 2009. Effect of changes in climate and emissions on future sulfate-nitrate-ammonium aerosol
881 levels in the United States. Journal of Geophysical Research-Atmospheres 114, D01205,
882 doi:10.1029/2008jd010701.

Revuelta, M. A., Harrison, R. M., Núñez, L., Gomez-Moreno, F. J., Pujadas, M., Artíñano, B., 2012. Comparison of temporal features of sulphate and nitrate at urban and rural sites in Spain and the UK. Atmospheric Environment 60, 383-391.

Rolph, G.D., 2013. Real-time Environmental Applications and Display sYstem (READY) Website (http://www.ready.noaa.gov). NOAA Air Resources Laboratory, College Park, MD.

Saarnio K., Aurela M., Timonen H., Saarikoski S., Teinila K., Makela T., Sofiev, M., Koskinen, J., Aalto, P. P., Kulmala, M., Kukkonen, J., Hillamo, R., 2010. Chemical composition of fine particles in fresh smoke plumes from boreal wild-land fires in Europe. Science of the Total Environment 408, 2527-2542.

Schaap, M., Spindler, G., Schulz, M., Acker, K., Maenhaut, W., Berner, A., et al., 2004a. Artefacts in the sampling of nitrate studied in the "INTERCOMP" campaigns of EUROTRAC-AEROSOL. Atmospheric Environment 38, 6487-6496.

Schaap, M., van Loon, M., ten Brink, H. M., Dentener, F. J., Builtjes, P. J. H., 2004b. Secondary inorganic aerosol simulations for Europe with special attention to nitrate. Atmospheric Chemistry and Physics 4, 857-874.

Seibert, P., Kromp-Kolb, H., Baltensperger, U., Jost, D. T., Schwikowski, M., 1994. Trajectory analysis of high-alpine air pollution data. In Air pollution modeling and its application X. Springer US, pp 595-596.

Seinfeld, J. H., Pandis, S. N., 2006. Atmospheric Chemistry and Physics, second ed. In: From Air Pollution to Climate Change John Wiley & Sons, NewYork.

Shi Z., Zhang D., Hayashi M., Ogata H., Ji H., Fujiie W., 2008. Influences of sulfate and nitrate on the hygroscopic behaviour of coarse dust particles. Atmospheric Environment 42(4), 822-827.

Squizzato S., Masiol M., Brunelli A., Pistollato S., Tarabotti E., Rampazzo G., Pavoni B., 2013. Factors determining the formation of secondary inorganic aerosol: a case study in the Po Valley (Italy). Atmospheric Chemistry and Physics 13, 1927-1939.

Squizzato, S., Masiol, M., Visin, F., Canal, A., Rampazzo, G., Pavoni, B., 2014. The PM2.5 chemical composition in an industrial zone included in a large urban settlement: main sources and local background. Environmental Science: Processes & Impacts 16, 1913-1922.

Stelson A. W. Seinfeld D. H., 1982. Relative humidity and temperature dependence of the ammonium nitrate dissociation constant. Atmospheric Environment 16, 983-992.
Stockwell, W. R., Calvert, J. G., 1983. The mechanism of the HO-SO2 reaction. Atmospheric Environment 17, 2231-2235.

Stohl, A., 1998. Computation, accuracy and applications of trajectories-a review and bibliography. Atmospheric Environment 32, 947-966.

931 Sutton, M. A., Erisman, J. W., Dentener, F., Möller, D., 2008. Ammonia in the environment:
932 From ancient times to the present. Environmental Pollution 156, 583-604.
933
934 Tositti L., Brattich E., Masiol M., Baldacci D., Ceccato D., Parmeggiani S., Stracquadanio,
935 M., Zappoli, S., 2014. Source apportionment of particulate matter in a large city of
936 southeastern Po Valley (Bologna, Italy). Environmental Science and Pollution Research 21,
937 872-890.
938
939 Vecchi, R., Marcazzan, G., Valli, G., Ceriani, M., Antoniazzi, C., 2004. The role of
940 atmospheric dispersion in the seasonal variation of PM1 and PM2.5 concentration and
941 composition in the urban area of Milan (Italy). Atmospheric Environment 38, 4437-4446.
942
943 Vecchi, R., Valli, G., Fermo, P., D'Alessandro, A., Piazzalunga, A., Bernardoni, V., 2009.
944 Organic and inorganic sampling artefacts assessment. Atmospheric Environment 43, 1713-
945 1720.
946
947 WHO, 2006. Air Quality Guidelines, Global Update 2005. World Health Organisation,
948 Geneva.
949
950 Wichink Kruit, R. J., Schaap, M., Sauter, F. J., van Zanten, M. C., van Pul, W. A. J., 2012.
951 Modeling the distribution of ammonia across Europe including bi-directional surface–
952 atmosphere exchange. Biogeosciences 9, 5261-5277.
953
954 Wu, S.-Y., Hu, J.-L., Zhang, Y., Aneja, V.P., 2008. Modeling atmospheric transport and fate
955 of ammonia in North Carolina e part II: effect of ammonia emissions on fine particulate
956 matter formation. Atmospheric Environment 42, 3437-3451.
957
958 Zhang, X. Q. McMurry, P.H., 1992. Evaporative loss of fine particulate nitrates during
959 sampling. Atmospheric Environment 26A, 3305–3312.

TABLE LEGENDS

Table 1. Characteristics of the selected sampling sites and the number of analysed samples.

Table 2. Annual average concentrations of analysed pollutants. A full list of results including monthly average concentrations is provided as supplementary material Table SI1.

Table 3. Inter-site correlation matrices. Upper-left: box-cox transformed $PM_{2.5}$ dataset for the whole year (365 day); other matrices are calculated on the selected periods (60 days) and data were monthly normalized. Only significant ($p<$ 0.05) correlations are shown; correlations significant ($p<0.01$) are bold faced. Correlation matrices for all analysed compounds is provided in Table SI2.

FIGURE LEGENDS

Figure 1. Map of selected sites (a; left) and annual average percentages of analysed ions on ΣWSII (b; right).

Figure 2. Time series of sulphate, nitrate and ammonium in the six sites.

Figure 3. Time series of neutralisation ratio (NR) in the six sites.

Figure 4. Scatterplots of a) ammonium vs NR and b) ionic balance vs NR. Samples collected in six sites are coloured differently.

Figure 5. Results of the back-trajectory clustering (upper) and distributions of $PM_{2.5}$ and ion concentrations for each identified cluster (bottom). Results for remaining ions are provided as Supplementary Information Figure SI6.

Figure 6a. CWT analysis for $PM_{2.5,}$ nitrate and sulphate. Concentrations are expressed as $\mu g\ m^{-3}$.

Figure 6b. CWT analysis for chloride, potassium and calcium. Concentrations are expressed as $\mu g\ m^{-3}$.

Figure 7. Single back-trajectories during three high-nitrate concentration events.

Table 1. Characteristics of the selected sampling sites and the number of analysed samples.

	Municipality	Latitude	Longitude	Alt (m)	Site characteristics	Other automatic measurements
BL	Belluno	46.143 N	12.218 E	401	Public park, residential-commercial area	SO_2; O_3; NO_2 ; NO ; NO_x ; CO ; Benzene ; PM_{10} (gravimetric); PM_{10} (BAMs)
TV	Conegliano	45.890 N	12.307 E	72	Residential area	SO_2 ; O_3 ; NO_2 ; NO ; NO_x ; CO ; PM_{10} (gravimetric)
VI	Vicenza	45.560 N	11.539 E	36	Residential area	NO_2 ; NO ; NO_x ; PM_{10} (gravimetric); PAHs
PD	Padova	45.371 N	11.841 E	13	Residential area	SO_2 ; O_3 ; NO_2 ; NO ; NO_x ; CO ; Benzene ; PM_{10} (gravimetric); PAHs
VE	Venice-Mestre	45.498 N	12.261 E	1	Public park, residential area	SO_2 ; O_3 ; NO_2 ; NO ; NO_x ; CO ; Benzene ; PM_{10} (gravimetric); PAHs
RO	Rovigo	45.074 N	11.782 E	7	Residential-commercial area	SO_2 ; TSP (gravimetric); O_3 ; NO_2 ; NO ; NO_x ; CO ; PM_{10} (gravimetric)

Table 2. Annual average concentrations of analysed pollutants. A full list of results including monthly average concentrations is provided as supplementary material Table SI1.

		BL	TV	VI	VE	PD	RO
$PM_{2.5}$	µg m^{-3}	17	20	28	25	29	27
Na^+	µg m^{-3}	0.14	0.31	0.15	0.16	0.47	0.23
NH_4^+	µg m^{-3}	0.9	1.1	2.3	1.9	2	2.3
K^+	µg m^{-3}	0.28	0.29	0.31	0.38	0.39	0.3
Ca^{2+}	µg m^{-3}	0.11	0.15	0.15	0.15	0.16	0.15
Cl^-	µg m^{-3}	0.12	0.12	0.19	0.17	0.19	0.24
NO_3^-	µg m^{-3}	1.8	2.4	5	3.6	4.6	5.2
SO_4^{2-}	µg m^{-3}	1.5	1.7	2.4	2.6	2.4	2.6
SIA	µg m^{-3}	4.2	5.2	9.7	8.1	9	10.2
SIA	%	23	25	32	30	29	35
ΣWSII	µg m^{-3}	5.2	6.5	10.8	9.2	10.7	11.4
ΣWSII	%	30	34	36	35	38	41
NO	µg m^{-3}	15	12	24	22	27	26
NO_2	µg m^{-3}	23	27	33	32	37	36
NO_x	µg m^{-3}	45	45	70	65	79	76
O_3	µg m^{-3}	49	47	48	49	61	46
SO_2	µg m^{-3}	1.1	—	—	2.8	1	2.5

Table 3. Inter-site correlation matrices. Upper-left: box-cox transformed $PM_{2.5}$ dataset for the whole year (365 day); other matrices are calculated on the selected periods (60 days) and data were monthly normalized. Only significant ($p < 0.05$) correlations are shown; correlations significant ($p<0.01$) are bold faced. Correlation matrices for all analysed compounds is provided in Table SI2.

$PM_{2.5}$ (Whole year)	**BL**	**TV**	**VI**	**VE**	**PD**	**RO**
BL	1					
TV	**0.74**	1				
VI	**0.75**	**0.86**	1			
VE	**0.75**	**0.82**	**0.86**	1		
PD	**0.74**	**0.83**	**0.89**	**0.94**	1	
RO	**0.71**	**0.82**	**0.88**	**0.9**	**0.93**	1

$PM_{2.5}$ (Monthly norm.)	**BL**	**TV**	**VI**	**VE**	**PD**	**RO**
BL	1					
TV	0.33	1				
VI	0.26	**0.84**	1			
VE		**0.84**	**0.89**	1		
PD	0.29	**0.85**	**0.89**	**0.87**	1	
RO	0.26	**0.8**	**0.81**	**0.83**	**0.95**	1

NO_3^- (Monthly norm.)	**BL**	**TV**	**VI**	**VE**	**PD**	**RO**
BL	1					
TV		1				
VI		**0.84**	1			
VE		**0.85**	**0.95**	1		
PD		**0.87**	**0.97**	**0.96**	1	
RO		**0.79**	**0.86**	**0.84**	**0.92**	1

SO_4^{2-} (Monthly norm.)	**BL**	**TV**	**VI**	**VE**	**PD**	**RO**
BL	1					
TV	**0.51**	1				
VI	**0.39**	**0.51**	1			
VE	**0.53**	**0.86**	**0.58**	1		
PD	**0.54**	**0.74**	**0.59**	**0.9**	1	
RO	**0.39**	**0.73**	**0.55**	**0.83**	**0.89**	1

NH_4^+ (Monthly norm.)	**BL**	**TV**	**VI**	**VE**	**PD**	**RO**
BL	1					
TV		1				
VI	0.26	**0.81**	1			
VE		**0.86**	**0.92**	1		
PD		**0.87**	**0.94**	**0.95**	1	
RO	0.26	**0.77**	**0.85**	**0.83**	**0.92**	1

K^+ (Monthly norm.)	**BL**	**TV**	**VI**	**VE**	**PD**	**RO**
BL	1					
TV		1				
VI		**0.58**	1			
VE		**0.64**	**0.82**	1		
PD		**0.51**	**0.83**	**0.77**	1	
RO		0.32	**0.52**	**0.56**	**0.77**	1

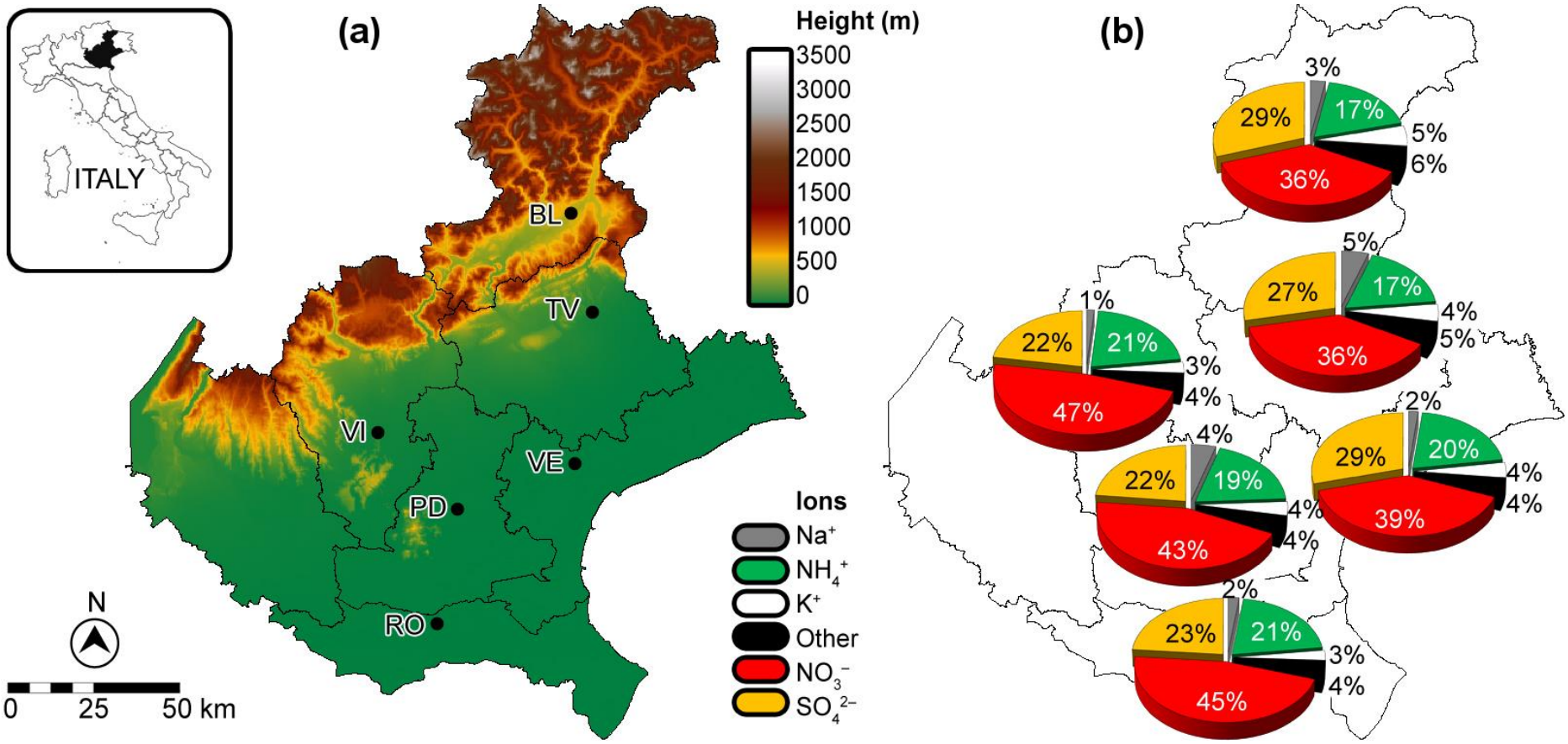

Figure 1. Map of selected sites (a; left) and annual average percentages of analysed ions on ΣWSII (b; right).

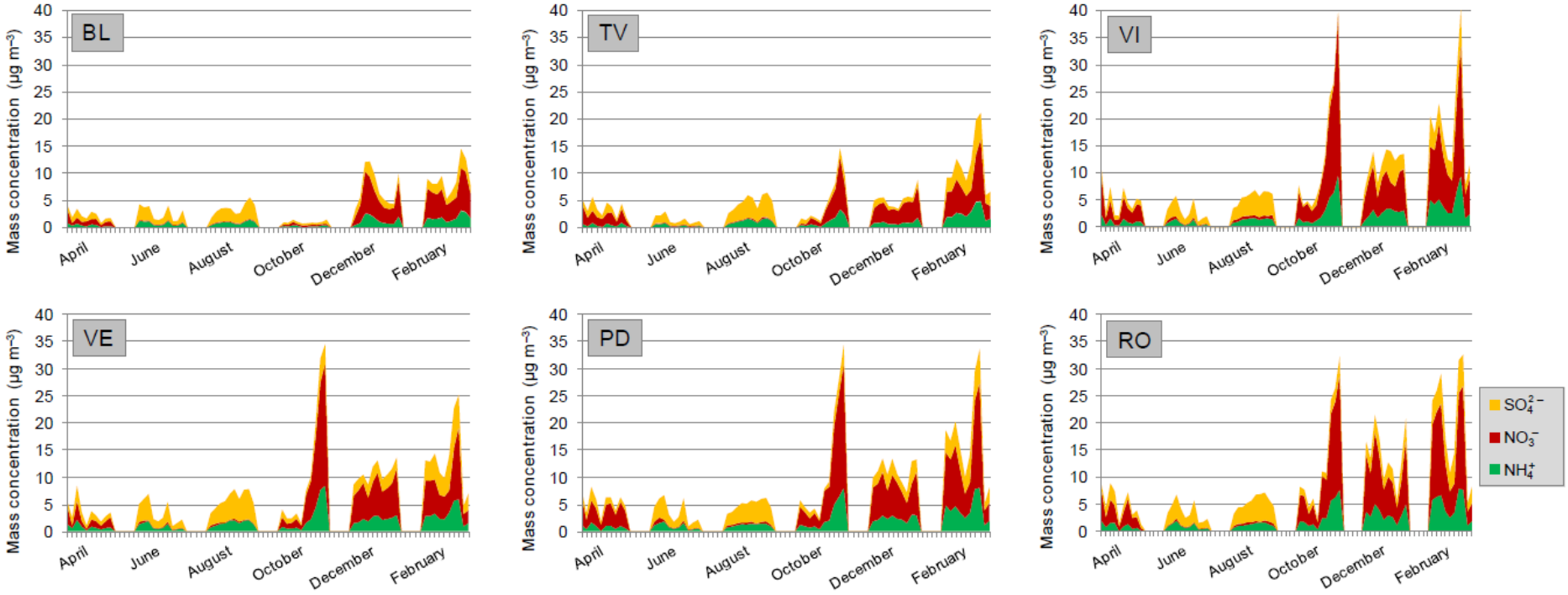

Figure 2. Time series of sulphate, nitrate and ammonium in the six sites.

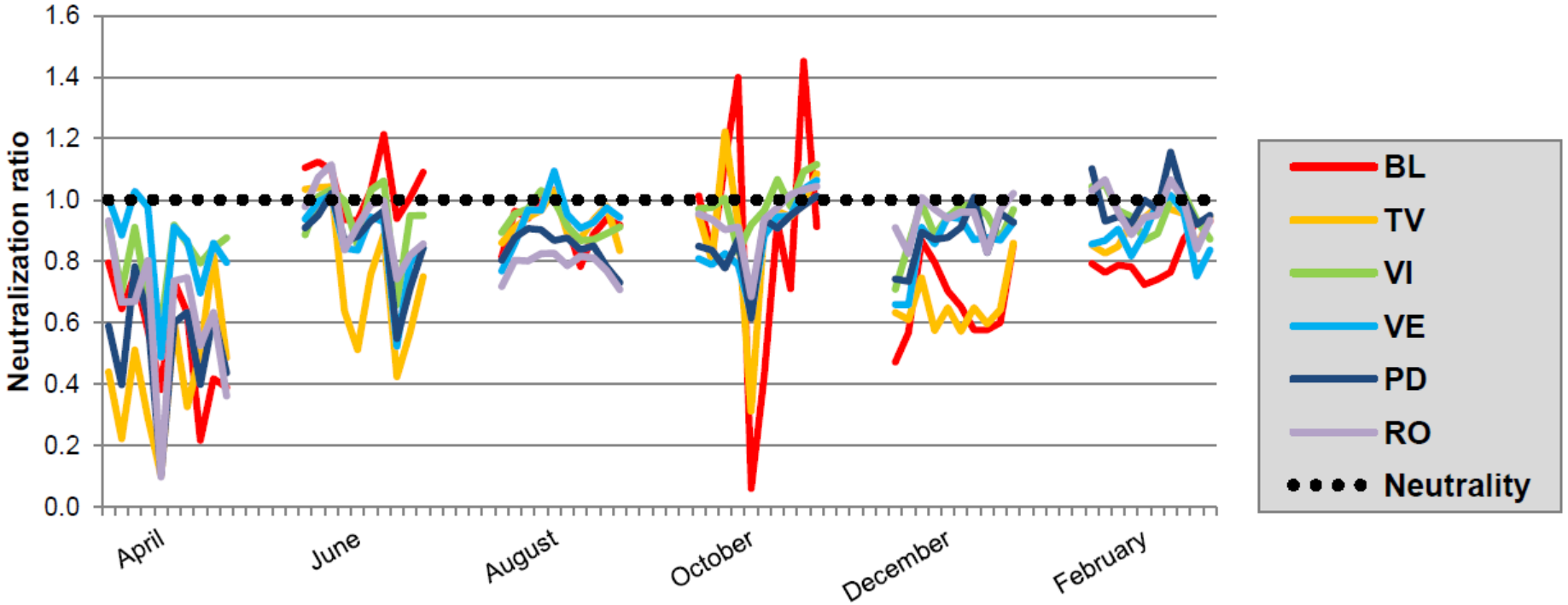

Figure 3. Time series of neutralisation ratio (NR) in the six sites.

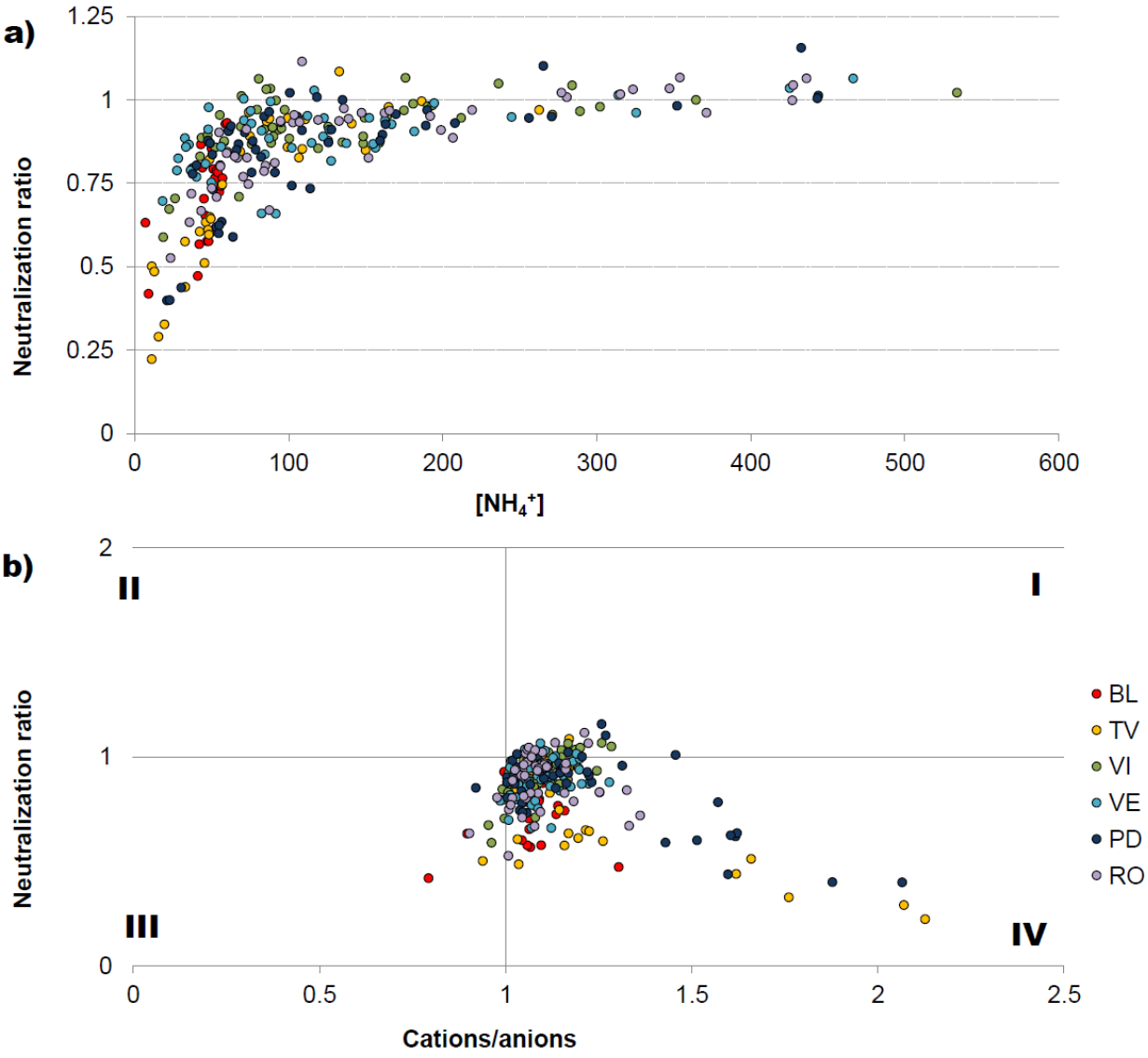

Figure 4. Scatterplots of a) ammonium vs NR and b) ionic balance vs NR. Samples collected in six sites are coloured differently.

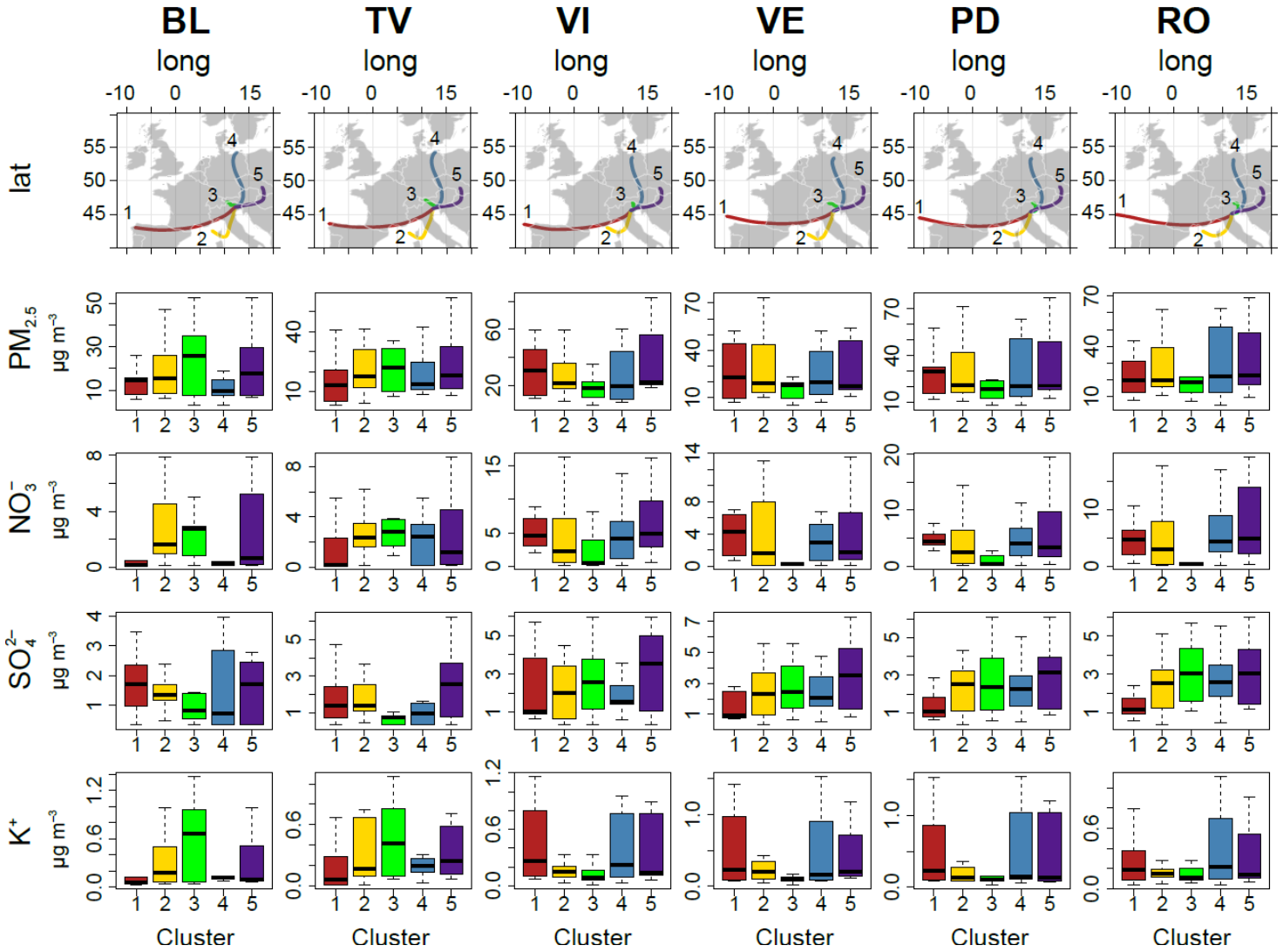

Figure 5. Results of the back-trajectory clustering (upper) and distributions of $PM_{2.5}$ and ion concentrations for each identified cluster (bottom). Results for remaining ions are provided as Supplementary Information Figure SI6.

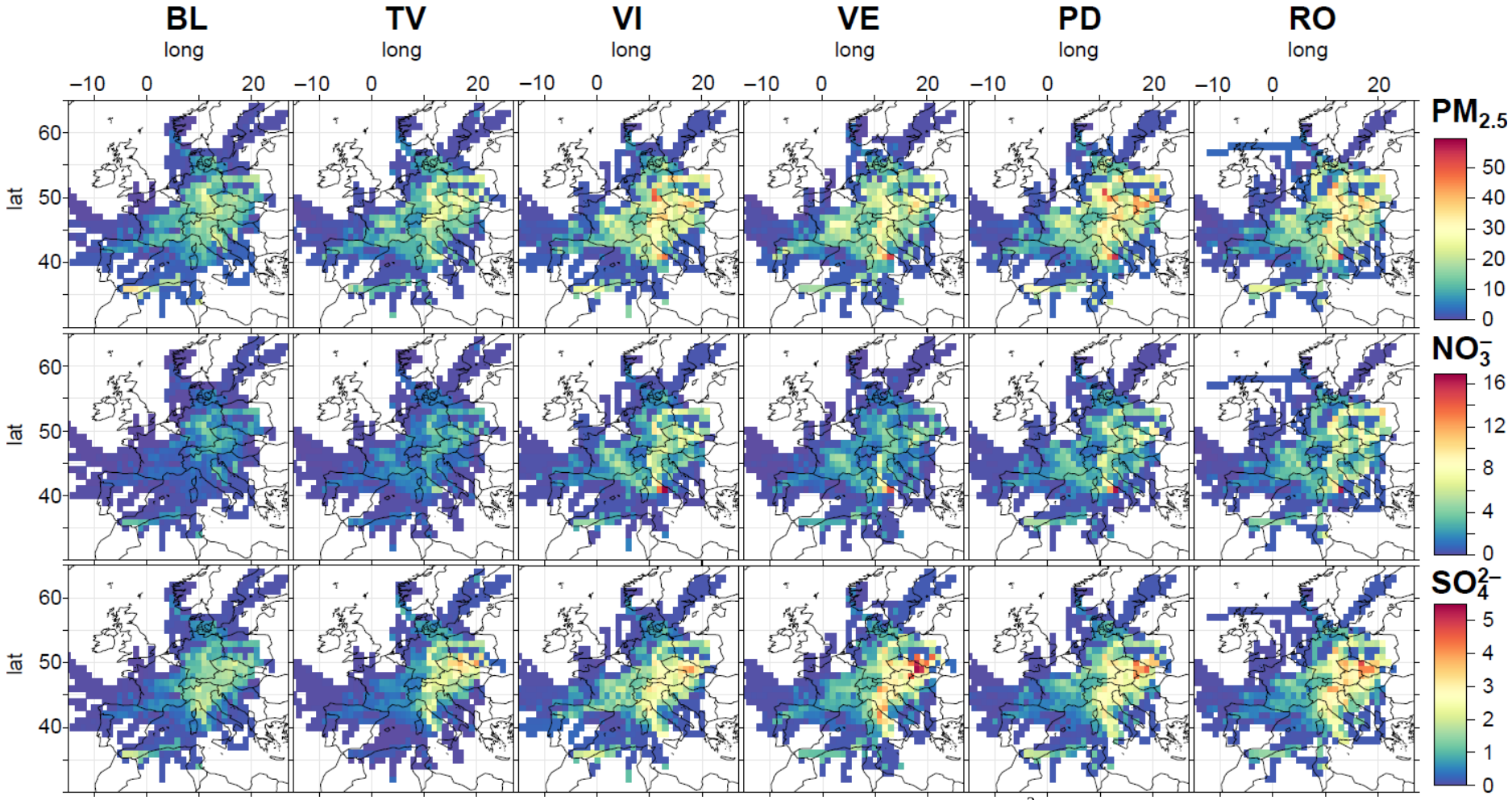

Figure 6a. CWT analysis for $PM_{2.5,}$ nitrate and sulphate. Concentrations are expressed as µg m^{-3}.

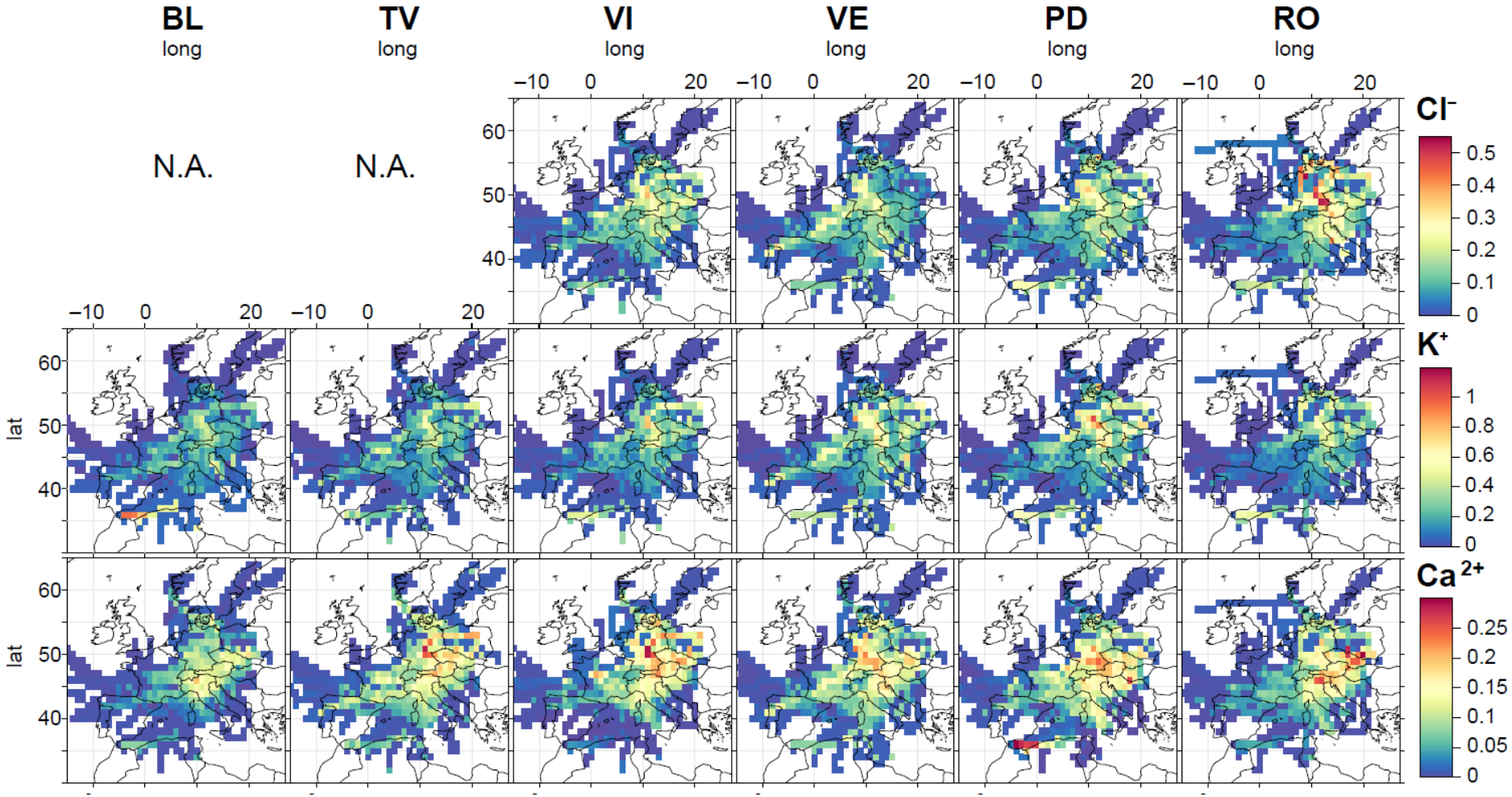

Figure 6b. CWT analysis for chloride, potassium and calcium. Concentrations are expressed as µg m^{-3}.

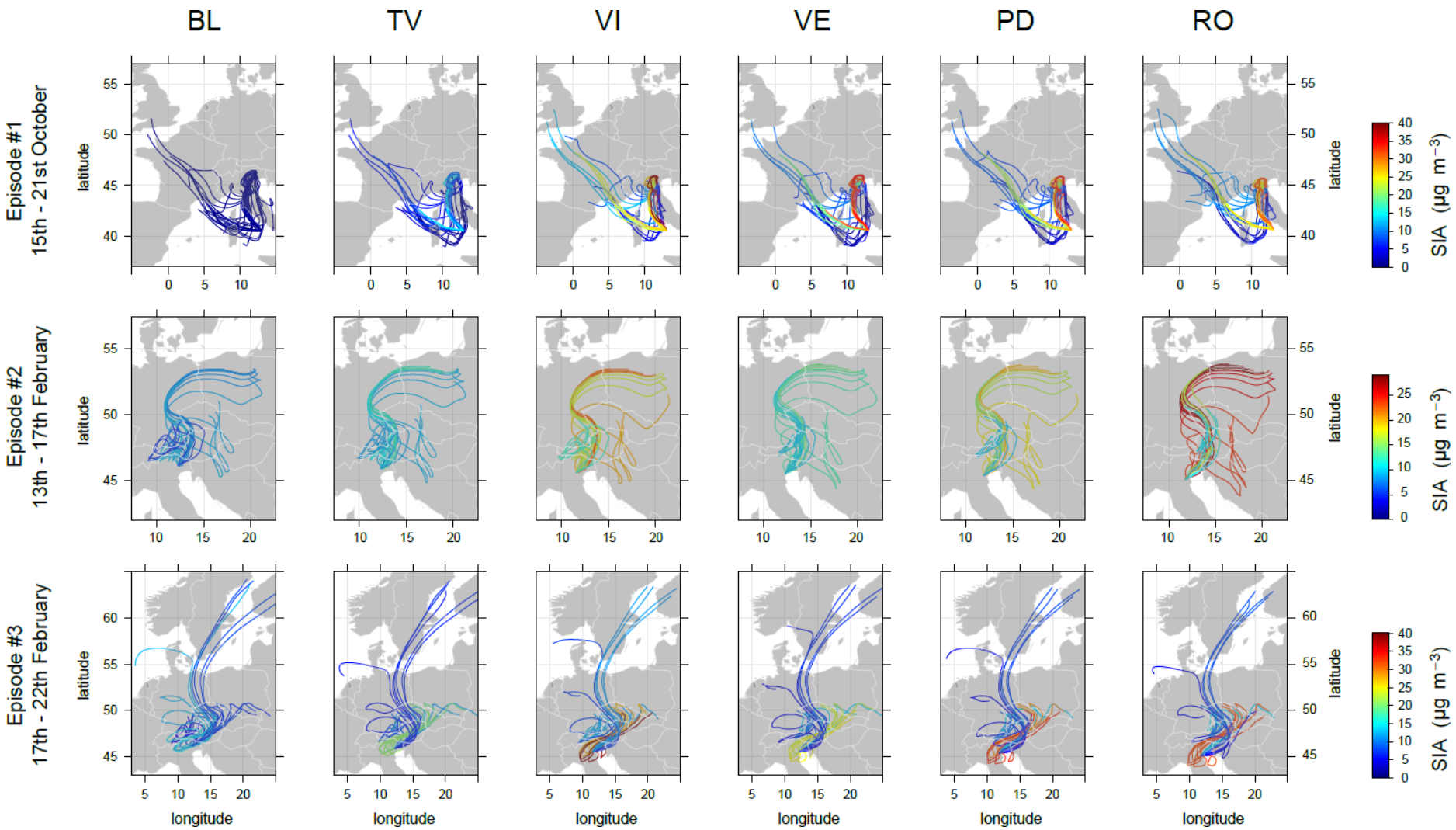

Figure 7. Single back-trajectories during three high-nitrate concentration events.

Graphical abstract